

Dynamics of an axisymmetric body spinning on a horizontal surface. I. Stability and the gyroscopic approximation

H. K. Moffatt, Y. Shimomura and M. Branicki

Proc. R. Soc. Lond. A 2004 **460**, doi: 10.1098/rspa.2004.1329, published 8 December 2004

References

Article cited in:

<http://rspa.royalsocietypublishing.org/content/460/2052/3643#related-urls>

Email alerting service

Receive free email alerts when new articles cite this article - sign up in the box at the top right-hand corner of the article or click [here](#)

Dynamics of an axisymmetric body spinning on a horizontal surface. I. Stability and the gyroscopic approximation

BY H. K. MOFFATT¹, Y. SHIMOMURA² AND M. BRANICKI¹

¹*Department of Applied Mathematics and Theoretical Physics, Wilberforce Road, Cambridge CB3 0WA, UK (hkm2@damtp.cam.ac.uk; mb388@damtp.cam.ac.uk)*

²*Department of Physics, Keio University, Hiyoshi, Yokohama 223-8521, Japan (yutaka@phys-h.keio.ac.jp)*

Received 14 November 2003; accepted 23 April 2004; published online 1 October 2004

The general spinning motion of an axisymmetric rigid body on a horizontal table is analysed, allowing for slip and friction at the point of contact P . Attention is focused on the case of spheroids (prolate or oblate), and particularly on spheroids whose density distribution is such that the centre-of-mass and centre-of-volume coincide. Four classes of fixed points (i.e. steady states) are identified, and the linear stability properties in each case are determined, assuming viscous friction at P . The governing dynamical system is six-dimensional. Trajectories of the system are computed, and are shown in projection in a three-dimensional subspace; these start near unstable fixed points and (in the case of viscous friction) end at stable fixed points. It is shown *inter alia* that a uniform prolate spheroid set in sufficiently rapid spinning motion with its axis horizontal is unstable, and its axis rises to a stable steady state, at either an intermediate angle or the vertical, depending on the initial angular velocity. These computations allow an assessment of the circumstances under which the condition described as ‘gyroscopic balance’ is realized. Under this condition, the evolution from an unstable to a stable state is greatly simplified, being described by a first-order differential equation. Oscillatory modes which are stable on linear analysis may be destabilized during this evolution, with consequential oscillations in the normal reaction R at the point of support. The computations presented here are restricted to circumstances in which R remains positive.

Keywords: rigid body dynamics; dynamical systems; instability; spinning spheroid; gyroscopic approximation; Jellett constant

1. Introduction

The problem of the rolling, spinning and slipping of an axisymmetric body (or ‘top’) on a horizontal table, with or without friction at the point of contact, has been studied for well over a century, and indeed the equations governing the behaviour have been known since the work of Euler (for a historical review, see Perry (1957)). It might be thought therefore that there is little more to be said on this very classical problem. Surprisingly however, all treatments taking due account of slipping and friction at the point of contact that we have been able to trace (Braams 1952; Cohen

1977; Del Campo 1955; Ebenfeld & Scheck 1995; Fokker 1952; Gray & Nickel 2000; Hugenholtz 1952; Kane & Levinson 1978; Mertens & De Corte 1978; Mertens *et al.* 1982; O'Brien & Synge 1954; Or 1994; Parkyn 1958) make the assumption that the portion of the body surface that makes contact with the table is spherical. This is perhaps a good approximation in consideration of the stability of spin about the vertical, or for a top with a sharpened point which can be locally approximated by a hemisphere (a 'spherical-tip' top), or for a nearly spherical body whose density distribution is such that its centre-of-mass is displaced along the axis of symmetry from its centre-of-volume (the so-called 'tippe top'); but it clearly fails to describe the behaviour of a body such as a spheroid when the axis of symmetry is inclined at an arbitrary angle to the vertical. In such a situation, the assumption of sphericity is plainly inadmissible.

A preliminary approach to this problem was briefly described by Moffatt & Shimomura (2002) (hereafter referred to as MS02), who discussed the familiar phenomenon of the rise to the vertical of a hard-boiled egg set in rapid spinning motion on a table. In that paper, the governing equations were simplified on the assumption that the friction is weak and the spin is large (so that the Coriolis force is dominant). Under this 'gyroscopic' assumption, a first-order differential equation for the inclination θ of the axis of symmetry was obtained, which, for the case of a prolate spheroid, did indeed describe the rise of the axis to the vertical. This rise was associated with the effect of the weak friction μ at the point of contact, and occurred on a 'slow' time-scale $O(\mu^{-1})$, irrespective of the nature of the frictional force ('dry' Coulomb friction, or 'wet' viscous friction).

Under this gyroscopic approximation, it was found that the scalar product of the angular momentum and the vector from the centre-of-mass O to the point of contact P was a constant of the motion. This constant was first obtained for the case of the spherical-tip top by Jellett (1872), and it has played a key role in some of the analyses of the tippe top that have been published (e.g. Hugenholtz 1952; O'Brien & Synge 1954). The fact that Jellett's invariant is still invariant for an arbitrary axisymmetric body under the gyroscopic approximation was, however, new, and it was this fact that led to a profound simplification of the problem.

As indicated by MS02, there are many aspects of the problem that are not covered by the gyroscopic approximation, and indeed it is only through study of the exact problem that the limits of validity of the gyroscopic approximation can be determined. This is the purpose of the present paper. In §§ 2 and 3, the basic equations are obtained in the form of a sixth-order nonlinear dynamical system, subject to the single constraint that the normal reaction R at the point P must remain positive. In § 4, the gyroscopic approximation is restated, and a direct proof of the existence of Jellett's invariant under this approximation is given. In § 5, we specialize to the case of a spheroid, which may be prolate or oblate; we suppose that the centre-of-mass coincides with the centre-of-volume, and that the density distribution within the body is axisymmetric, but otherwise arbitrary. Four distinct classes of steady motion (fixed points in the phase-space) are identified, and in § 6, a linear stability analysis for each of these types of motion is presented. It is shown that the weakly unstable (or 'slow') mode for the case of a prolate spheroid set in precessional motion with $\theta = \pi/2$ is indeed governed by the gyroscopic approximation; other oscillatory modes are stable in linear analysis. The stability analysis guides the choice of numerical simulations presented in § 7, which show trajectories of the system evolving from unstable to

stable states, and which provide further evidence for the validity of the gyroscopic approximation over a significant range of parameters. The paper is summarized, and some open issues indicated, in the concluding section.

In all the computations presented here, the normal reaction R does remain positive, and the spheroid does therefore remain in contact with the table throughout the motion. However, there are circumstances (in particular, high aspect ratio and high initial angular momentum) when oscillatory modes can grow to such an extent that R can fall to zero. This can lead to a ‘jumping’ phenomenon, in which the body obviously passes into a different dynamical regime. This is an interesting and complex phenomenon, which will be the subject of a subsequent paper (part II).

2. Geometry and kinematics of the problem

Consider a rigid body of revolution with surface S that spins on a horizontal table with instantaneous point of contact P (figure 1). Let O be the centre-of-mass of the body and Oz its axis of symmetry. The lines Oz and OP in general define a vertical plane Π which also contains the upward vertical axis OZ. Let (θ, φ, ψ) be the Euler angles of the body relative to OZ, and let

$$\Lambda = \dot{\theta}, \quad \Omega = \dot{\varphi}, \quad n = \dot{\psi} + \Omega \cos \theta. \quad (2.1)$$

Thus, Λ is the rate of change of inclination of the axis of symmetry to the vertical, Ω the rate of precession of the plane Π about the vertical, and n the spin about the axis of symmetry Oz.

Let $Oxyz$ be the ‘body’ frame of reference, with Ox in the plane Π , and let $OXYZ$ be an alternative rotating frame with OX horizontal in the plane Π . The position vector of the body relative to O may then be written

$$\mathbf{x} = x\mathbf{i} + y\mathbf{j} + z\mathbf{k} = X\mathbf{I} + Y\mathbf{J} + Z\mathbf{K}, \quad (2.2)$$

where

$$x = X \cos \theta - Z \sin \theta, \quad y = Y, \quad z = X \sin \theta + Z \cos \theta, \quad (2.3)$$

and the unit vectors $(\mathbf{i}, \mathbf{j}, \mathbf{k})$ and $(\mathbf{I}, \mathbf{J}, \mathbf{K})$ are related by

$$\mathbf{i} = \mathbf{I} \cos \theta - \mathbf{K} \sin \theta, \quad \mathbf{j} = \mathbf{J}, \quad \mathbf{k} = \mathbf{I} \sin \theta + \mathbf{K} \cos \theta. \quad (2.4)$$

The frames $OXYZ$, $Oxyz$ rotate with respective angular velocities

$$\boldsymbol{\Omega} = \Omega \mathbf{K} = -\Omega \sin \theta \mathbf{i} + \Omega \cos \theta \mathbf{k}, \quad \boldsymbol{\Omega}' = \boldsymbol{\Omega} + \Lambda \mathbf{j}, \quad (2.5)$$

and the angular velocity of the body is

$$\boldsymbol{\omega} = -\Omega \sin \theta \mathbf{i} + \Lambda \mathbf{j} + n \mathbf{k}. \quad (2.6)$$

Let $h(\theta)$ be the height of O above the table; then, from consideration of the effect of a small change $\delta\theta$ in orientation of the body relative to the plane of the table, the coordinates (in $OXYZ$) of the point of contact P are given by

$$\mathbf{X}_P = (X_P, Y_P, Z_P) = (h'(\theta), 0, -h(\theta)), \quad (2.7)$$

and correspondingly, from (2.3),

$$x_P = -h^2 \frac{d}{d\theta} \left(\frac{\cos \theta}{h} \right), \quad z_P = -h^2 \frac{d}{d\theta} \left(\frac{\sin \theta}{h} \right). \quad (2.8)$$

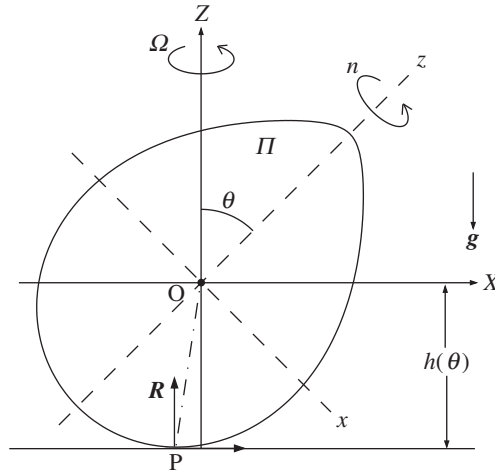


Figure 1. An axisymmetric body with centre-of-mass O spins on a horizontal table with point of contact P . Its axis of symmetry Oz and the axis OZ define a plane Π (containing OP) which precesses about OZ with angular velocity Ω . $OXYZ$ is a rotating frame of reference, with OX horizontal in the plane Π . The height of O above the table is $h(\theta)$ and the coordinates of P are $X_P = dh/d\theta$, $Y_P = 0$, $Z_P = -h(\theta)$. The forces acting on the body are its weight $-Mg\mathbf{K}$, the normal reaction \mathbf{R} at P , and the (horizontal) frictional force \mathbf{F} at P .

The function $h(\theta)$ is in principle determined by the shape of S and the position of O within S , and is clearly a continuous function of θ ($0 \leq \theta \leq \pi$). If S is everywhere convex, then $X_P = h'(\theta)$ also varies continuously with θ ; but if S is not everywhere convex, then $h'(\theta)$ has discontinuities when, as θ varies, the point of contact P jumps between two distinct points of S having a common tangent plane that is instantaneously coincident with the table.

Let $\mathbf{U} = U\mathbf{I} + V\mathbf{j} + W\mathbf{K}$ be the velocity of the centre-of-mass O . The velocity of the point P (of the body) is then

$$\mathbf{U}_P = \mathbf{U} + \boldsymbol{\omega} \wedge \mathbf{X}_P = U_P\mathbf{I} + V_P\mathbf{j} + W_P\mathbf{K}, \quad (2.9)$$

where

$$U_P = U - h\Lambda, \quad V_P = V + x_P(n - \Omega \cos \theta) + \Omega h'(\theta), \quad W_P = W - \Lambda h'(\theta). \quad (2.10)$$

Since $W_P = 0$ for as long as the body remains in contact with the table, we have

$$W = \Lambda h'(\theta). \quad (2.11)$$

Since we allow for slip however, U_P and V_P are in general non-zero.

Example 2.1 (spheroid of axisymmetric mass distribution). The case of a spheroid of axisymmetric mass distribution is a useful prototype which will be studied in some detail in this paper. If the mass distribution is non-uniform, then its centre-of-mass may be displaced a distance d , say, from its centre-of-volume. The equation of S is then

$$a^2(x^2 + y^2) + b^2(z - d)^2 = a^2b^2, \quad (2.12)$$

where $a/b \geq 1$ according as the spheroid is prolate or oblate. The function $h(\theta)$ is found from the condition that the plane $Z = -h$ is tangent to S , in the form

$$h(\theta) = (a^2 \cos^2 \theta + b^2 \sin^2 \theta)^{1/2} + d \cos \theta. \quad (2.13)$$

The following two cases should be noted.

- (i) If $d = 0$, i.e. the centre-of-mass coincides with the centre-of-volume, then

$$h(\theta) = (a^2 \cos^2 \theta + b^2 \sin^2 \theta)^{1/2}, \quad (2.14)$$

and then, from (2.7),

$$X_P = \frac{(b^2 - a^2) \sin 2\theta}{2h}, \quad Z_P = -h, \quad (2.15)$$

and, from (2.8),

$$x_P = \frac{b^2 \sin \theta}{h}, \quad z_P = -\frac{a^2 \cos \theta}{h}. \quad (2.16)$$

The expression (2.10)₂ for V_P reduces in this case to

$$V_P = V + x_P(n - (a/b)^2 \Omega \cos \theta). \quad (2.17)$$

- (ii) If $a = b$ and $d \neq 0$ (sphere with displaced centre-of-mass), then

$$h(\theta) = b + d \cos \theta. \quad (2.18)$$

This includes the case of the tippe top, which has been widely studied (see references cited in §1). It also covers the case of any ‘spherical-tip’ top for which the portion of the surface in contact with the table can be assumed to be part of a sphere (b then being the radius of this sphere and d the distance of its centre from the centre-of-mass of the top).

3. Dynamical equations

From this point on, we use dimensionless variables with $(M, b, (b/g)^{1/2})$ as the units of mass, length and time, where M is the mass of the body, b the radius of its section in the plane Oxy , and g the acceleration due to gravity. (Equivalently, we formally set $M = b = g = 1$.) The forces acting on the body are its weight $-\mathbf{K}$ at O , and the normal reaction $\mathbf{R} = R\mathbf{K}$ and frictional force $\mathbf{F} = F_X\mathbf{I} + F_Y\mathbf{j}$ at P . This frictional force depends on the physical properties of the two surfaces in contact; for the moment, we need merely assume that \mathbf{F} resists the slipping motion, so that

$$\mathbf{F} \cdot \mathbf{U}_P \leq 0. \quad (3.1)$$

The momentum equation, in an inertial frame of reference, is

$$\frac{d\mathbf{U}}{dt} = -\mathbf{K} + \mathbf{R} + \mathbf{F}. \quad (3.2)$$

Moreover, the angular momentum relative to O is $\mathbf{H} = \hat{\mathbf{I}} \cdot \boldsymbol{\omega}$, where $\hat{\mathbf{I}}$ is the inertia tensor at O , and the angular momentum equation, in the same inertial frame, is

$$\frac{d\mathbf{H}}{dt} = \mathbf{X}_P \wedge (\mathbf{R} + \mathbf{F}). \quad (3.3)$$

The energy of the body (kinetic plus potential) is

$$E = \frac{1}{2}\mathbf{U} \cdot \mathbf{U} + \frac{1}{2}\boldsymbol{\omega} \cdot \mathbf{H} + h(\theta), \quad (3.4)$$

and the energy equation derived in a standard way from (3.2) and (3.3) is

$$\frac{dE}{dt} = \mathbf{U}_P \cdot \mathbf{F} \leq 0. \quad (3.5)$$

Energy is dissipated solely through slipping and the associated friction at P.

In the rotating frame OXYZ, (3.2) becomes

$$\left(\frac{\partial \mathbf{U}}{\partial t} \right)_{\text{OXYZ}} + \boldsymbol{\Omega} \wedge \mathbf{U} = -\mathbf{K} + \mathbf{R} + \mathbf{F}, \quad (3.6)$$

with components

$$\dot{U} = \Omega V + F_X, \quad \dot{V} = -\Omega U + F_y, \quad \dot{W} = R - 1, \quad (3.7)$$

and we recall that $W = \Lambda h'(\theta)$. As regards (3.3), it is more convenient to use the body frame Oxyz in which $\hat{\mathbf{I}}$ is diagonalized, with diagonal elements (the principal moments of inertia) A, A, C . In this frame

$$\mathbf{H} = -A\Omega \sin \theta \mathbf{i} + A\Lambda \mathbf{j} + Cn \mathbf{k}, \quad (3.8)$$

and (3.3) becomes

$$\left(\frac{\partial \mathbf{H}}{\partial t} \right)_{\text{Oxyz}} + \boldsymbol{\Omega}' \wedge \mathbf{H} = \mathbf{X}_P \wedge (\mathbf{R} + \mathbf{F}), \quad (3.9)$$

with components

$$\left. \begin{aligned} A\dot{\Omega} \sin \theta + (2A\Omega \cos \theta - Cn)\Lambda &= z_P F_y, \\ A\dot{\Lambda} + \Omega \sin \theta (Cn - A\Omega \cos \theta) &= -RX_P + Z_P F_X, \\ C\dot{n} &= x_P F_y. \end{aligned} \right\} \quad (3.10)$$

The sets of equations (3.7) and (3.10) together with the defining equation $\Lambda = \dot{\theta}$ constitute a sixth-order nonlinear autonomous dynamical system in the variables

$$\Xi = (U, V, \Omega, \Lambda, \theta, n), \quad (3.11)$$

which we may arrange in the standard form $\dot{\Xi} = \mathcal{F}(\Xi)$:

$$\left. \begin{aligned} \dot{U} &= \Omega V + F_X, \\ \dot{V} &= -\Omega U + F_y, \\ \dot{\Omega} &= \frac{-2\Omega \Lambda \cos \theta + (C/A)n\Lambda + z_P F_y/A}{\sin \theta}, \\ \dot{\Lambda} &= \frac{\Omega \sin \theta (A\Omega \cos \theta - Cn) - RX_P + Z_P F_X}{A}, \\ \dot{\theta} &= \Lambda, \\ \dot{n} &= \frac{x_P F_y}{C}. \end{aligned} \right\} \quad (3.12)$$

Here X_P, Z_P, x_P and z_P are given by (2.7) and (2.8).

The normal reaction R is given, from (3.7), by

$$R = 1 + \dot{W} = 1 + \frac{d(\Lambda h'(\theta))}{dt}, \quad (3.13)$$

and this may be expressed, via (3.12), as a function

$$\begin{aligned} R &= R(U, \Omega, \Lambda, \theta, n) \\ &= \frac{1 + h''\Lambda^2 + h'\Omega \sin \theta (\Omega \cos \theta - Cn/A)}{1 + h'(h' - \mu h U_P)/A}, \end{aligned} \quad (3.14)$$

for the case of viscous friction (see (5.7)). The dynamical model holds only for so long as the condition $R \geq 0$ is satisfied. To complete the specification of the problem, \mathbf{F} must be prescribed in terms of R and \mathbf{U}_P (as given by (2.9) and (2.10)).

4. The gyroscopic approximation and the Jellett invariant

In the approach described by MS02, attention was focused on the high-spin situation, in which Coriolis effects dominate over both frictional and gravitational effects and the inclination θ in consequence changes slowly with time. In these circumstances, (3.10)₂ degenerates at leading order to

$$Cn - A\Omega \cos \theta = 0, \quad (4.1)$$

a state that we describe as one of ‘gyroscopic balance’. In this state, the kinetic energy is much greater than the potential energy.

It was then shown (MS02) that under this gyroscopic approximation and using (4.1), the quantity

$$J = -\mathbf{H} \cdot \mathbf{X}_P = A\Omega h \quad (4.2)$$

is constant, independently of the nature of the frictional force \mathbf{F} . This may be seen directly as follows. Using (3.3), we have $\mathbf{X}_P \cdot d\mathbf{H}/dt = 0$, so that

$$\frac{dJ}{dt} = -\mathbf{H} \cdot \frac{d\mathbf{X}_P}{dt}. \quad (4.3)$$

Now $\mathbf{X}_P = h'(\theta)\mathbf{I} - h(\theta)\mathbf{K}$, so that

$$\frac{d\mathbf{X}_P}{dt} = \left(\frac{\partial \mathbf{X}_P}{\partial t} \right)_{\text{OXYZ}} + \boldsymbol{\Omega} \wedge \mathbf{X}_P = h''(\theta)\dot{\theta}\mathbf{I} + (\Omega\mathbf{J} - \dot{\theta}\mathbf{K})h'(\theta) \quad (4.4)$$

and hence

$$\frac{dJ}{dt} = (A\Omega \cos \theta - Cn)(h'' \sin \theta - h' \cos \theta)\dot{\theta} = (Cn - A\Omega \cos \theta)h'^2 \frac{d}{dt} \left(\frac{\sin \theta}{h'} \right). \quad (4.5)$$

Thus, if the gyroscopic condition (4.1) is satisfied, then $dJ/dt = 0$, and $J = \text{const}$. Since (4.1) is at best a ‘high-spin’ approximation, this constant should be regarded as an adiabatic invariant, constant on a time-scale determined by the relatively weak effect of friction at P: we would expect that $J^{-1}dJ/dt \ll \mu \ll 1$; some supporting evidence is provided by the numerical simulations in § 7.

The result (4.5) shows that J is also constant if $d(\sin \theta/h')/dt = 0$, i.e. if

$$h(\theta) = b + d \cos \theta, \quad (4.6)$$

where b and d are constants. This is the special case (2.18) of a spherical-tip top, for which the constant J was first identified by Jellett (1872). We continue to describe it as Jellett's constant in the distinct context of non-spherical bodies of revolution in gyroscopic balance.

The fact that the behaviour is to some extent controlled by Jellett's constant (rather than by constancy of angular momentum) provides useful insight into certain aspects of observed behaviour. Recall that, for the well-known Euler problem of a body spinning freely in space and subject to weak dissipation due to the presence of viscous fluid in a small internal cavity, angular momentum is conserved and the body will spin ultimately about its axis of greatest moment of inertia, thus minimizing kinetic energy for the (prescribed) angular momentum. For a uniform prolate spheroid, this axis is perpendicular to the axis of symmetry; for a uniform oblate spheroid it coincides with the axis of symmetry.

By contrast, when the body spins on a table with weak friction at the point of contact and under the condition of gyroscopic balance, it is Jellett's constant J that should be 'prescribed'. Thus, for example, if a uniform spheroid (for which $A = \frac{1}{5}(a^2 + 1)$, $C = \frac{2}{5}$) spins in the orientation $\theta = \pi/2$ with angular velocity Ω , then (with $b = 1$) $J = A\Omega$, and the (dominant) kinetic energy is given by

$$T_{\pi/2} = \frac{1}{2}A\Omega^2 = \frac{J^2}{2A}. \quad (4.7)$$

If it spins in the orientation $\theta = 0$ with spin n , then $J = Cna$ and the kinetic energy is

$$T_0 = \frac{1}{2}Cn^2 = \frac{J^2}{2Ca^2}. \quad (4.8)$$

Hence

$$\frac{T_0}{T_{\pi/2}} = \frac{A}{Ca^2} = \frac{a^2 + 1}{2a^2}. \quad (4.9)$$

For a prolate spheroid ($a > 1$) the orientation $\theta = 0$ is preferred (the energy then being minimal), while for an oblate spheroid ($a < 1$) the orientation $\theta = \pi/2$ is preferred. This is just the opposite of the situation for the free-rotation problem.

These results are familiar from 'toy' experiments: when a hard-boiled egg is rapidly spun on a table, it will rise to spin on one end, whereas when a pebble as used in the Chinese game of 'Go' (near enough an oblate spheroid) is spun on a table about its axis of symmetry, it will rise to spin on its rim. In both these cases, potential energy increases, but this is more than compensated by the decrease in the (dominant) kinetic energy.

5. Steady states for the case of a spheroid

To be specific, we focus henceforth on the case of a spheroid whose density distribution is such that its centre-of-mass coincides with its centre-of-volume, so that (now with $b = 1$)

$$h(\theta) = Z_P = (a^2 \cos^2 \theta + \sin^2 \theta)^{1/2} \quad (5.1)$$

and, from (2.17),

$$V_P = V + x_P(n - a^2\Omega \cos \theta). \quad (5.2)$$

Such a geometry, for which $h(\pi - \theta) = h(\theta)$ may be described as ‘flip symmetric’. (The situation when $h(\pi - \theta) \neq h(\theta)$ introduces qualitative differences, which will be treated in a separate paper.) The dynamical characteristics of the spheroid are its principal moments of inertia (A, C) at O, which depend on the density distribution within the body (assumed axisymmetric). The following three cases are worth noting.

(i) Uniform spheroid:

$$A = \frac{1}{5}(a^2 + 1), \quad C = \frac{2}{5}; \quad (5.3)$$

(ii) ‘Polar’ spheroid, for which half of the mass is concentrated at each pole:

$$A = a^2, \quad C = 0; \quad (5.4)$$

(iii) ‘Equatorial’ spheroid, for which the mass is uniformly concentrated on a hoop round the equator:

$$A = \frac{1}{2}, \quad C = 1. \quad (5.5)$$

Note that for any axisymmetric density distribution, $A/C \geq \frac{1}{2}$.

In order to make progress, we must also specify the relationship between the frictional force \mathbf{F} and the slip velocity \mathbf{U}_P . Here, there are two possible standard choices.

(i) Dry (or ‘Coulomb’) friction, for which

$$\mathbf{F} = \mathbf{F}^{(c)} = -\frac{\mu R \mathbf{U}_P}{|\mathbf{U}_P|}, \quad (5.6)$$

where μ is a (dimensionless) coefficient of friction. This law is realistic provided $|\mathbf{U}_P|$ is bounded away from zero, but fails in a neighbourhood of $\mathbf{U}_P = \mathbf{0}$ where (5.6) is non-analytic. In particular it cannot be used for stability analysis of steady states, at which, necessarily, $\mathbf{U}_P = \mathbf{0}$ (see the energy equation (3.5)).

(ii) Wet (or ‘viscous’) friction, for which

$$\mathbf{F} = \mathbf{F}^{(v)} = -\mu R \mathbf{U}_P, \quad (5.7)$$

where μ is again a coefficient of friction (but now having dimensions (velocity)⁻¹ when we return to dimensional variables). This law is approximately realized in practice if there is a thin layer of oil or other lubricating fluid between the spheroid and the table. (Friction due to pure rotation about the normal at P will be ignored.) It has the great advantage of analyticity near $\mathbf{U}_P = \mathbf{0}$ and provides a plausible model for analysis of the stability of steady states.

The steady states of the system (3.12) are the fixed points where

$$\dot{\boldsymbol{\Xi}} = \mathcal{F}(\boldsymbol{\Xi}) = 0. \quad (5.8)$$

We adopt the viscous law (5.7) so that the energy equation becomes

$$\frac{dE}{dt} = -\mu R \mathbf{U}_P^2. \quad (5.9)$$

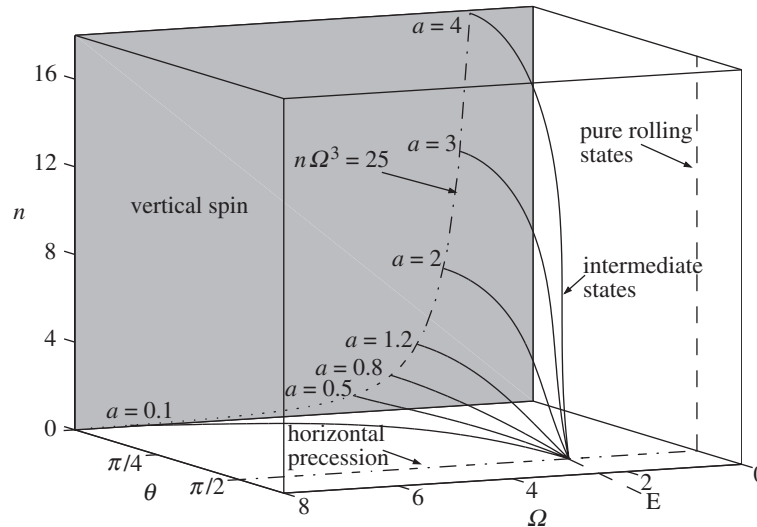


Figure 2. Fixed-points of the dynamical system (3.12) for a uniform spheroid in the three-dimensional subspace (Ω, θ, n) of the six-dimensional phase space $\Xi = (U, V, \Omega, \Lambda, \theta, n)$. The solid curves are the sets of intermediate steady states, which depend on the aspect ratio a ; these curves all pass through the point E (where $\Omega = \sqrt{5}$) and terminate on the shaded plane $\theta = 0$ at points on the curve $n\Omega^3 = 25$, and are there tangent to the planes $n = \sqrt{5}a^3$. The dot-dashed line represents states of horizontal precession, and the vertical dashed line is a projection into the subspace of pure rolling states. Note that all fixed points are non-isolated.

Hence, in a steady state with $\mu > 0$, it follows that $\mathbf{U}_P = \mathbf{0}$ and $\mathbf{F} = \mathbf{0}$. From (3.7) with $\mathbf{U} = \mathbf{0}$, we then have $R = 1$ and $\Omega U = \Omega V = 0$. Also $\Lambda(=\dot{\theta}) = 0$ in a steady state, so from (2.11) $W = 0$ also; moreover, from (5.2)

$$V + x_P(n - a^2\Omega \cos \theta) = 0, \quad (5.10)$$

and from (3.12)₄

$$(A\Omega \cos \theta - Cn)\Omega \sin \theta = X_P. \quad (5.11)$$

These equations have the following obvious solutions (see figure 2, in which they are represented in the three-dimensional subspace (Ω, θ, n) of the six-dimensional phase space $\Xi = (U, V, \Omega, \Lambda, \theta, n)$).

(a) *Vertical spin states*

$$U = V = \theta = \Lambda = 0, \quad n \text{ arbitrary}, \quad \Omega \text{ undefined}, \quad (5.12)$$

representing spin about the axis of symmetry in the vertical orientation.

(b) *Horizontal precession states*

$$\theta = \frac{1}{2}\pi, \quad U = V = \Lambda = n = 0, \quad \Omega \text{ arbitrary}, \quad (5.13)$$

representing a motion in which the axis of symmetry rotates in a horizontal plane with precessional angular velocity Ω . These states are represented by the dot-dashed line in figure 2.

(c) Intermediate states

These are steady states for which $U = V = \Lambda = 0$ and $0 < \theta < \frac{1}{2}\pi$ (so $x_P \neq 0$); for such states,

$$n = a^2 \Omega \cos \theta, \quad (5.14)$$

and (5.11) becomes

$$\Omega^2 = D((a^2 - 1) \cos^2 \theta + 1)^{-1/2}, \quad (5.15)$$

where

$$D = \frac{a^2 - 1}{a^2 C - A}. \quad (5.16)$$

The condition for the existence of such states is evidently $D > 0$, or equivalently

$$a^2 C \gtrless A \text{ for prolate/oblate spheroids,} \quad (5.17)$$

and there is then, for given θ , a unique pair (Ω, n) with $\Omega > 0, n > 0$ given by (5.14) and (5.15). Note that for the case (5.3) of a uniform spheroid $D = 5$, so that such intermediate states exist for all values of a ; these are represented by the solid curves of figure 2. These curves terminate on the shaded plane $\theta = 0$ at points on the curve $n\Omega^3 = 25$, and are there tangent to the plane $n = \sqrt{5}a^3$. (For the polar spheroid (5.4), $D = (1 - a^2)/a^2$, positive only if the spheroid is oblate ($a < 1$); and for the equatorial spheroid (5.5), $D = (a^2 - 1)/(a^2 - \frac{1}{2})$, positive for $a^2 > 1$ or $a^2 < \frac{1}{2}$.)

(d) Pure rolling states

Finally, there are also ‘pure rolling states’ for which n is arbitrary, and

$$\theta = \frac{1}{2}\pi, \quad V = -n, \quad U = \Omega = \Lambda = 0. \quad (5.18)$$

The vertical dashed line in figure 2 represents the projection of these pure rolling states into the three-dimensional subspace.

Note that each of these four categories of steady states is represented by a continuous line or curve in phase-space, and that all fixed points are non-isolated. This means that neutrally stable perturbations to neighbouring steady states are always possible; such (trivial) perturbations may be ignored in the following stability analysis.

6. Stability of the steady states

In order to analyse the stability of the steady states identified above, we shall continue to use the viscous friction model (5.7), which permits analytical treatment. This analysis will help in the interpretation of the computed trajectories of the system that follows in §7. These trajectories may be computed for either viscous friction or Coulomb friction; as recognized by Kane & Levinson (1978) for the case of a spherical-tip top, the dependence on the friction parameter μ may be expected to be qualitatively different in these two cases.

(a) Stability of vertical spin

The state of vertical spin is, in some sense, degenerate, because Ω is undefined in this state. Nevertheless, the linear stability of this state may be analysed as follows.

When θ is small, (2.15) and (2.16) give (with $b = 1$)

$$Z_P = -a + \frac{1}{2}c\theta^2 + O(\theta^4), \quad (6.1)$$

where $c = -h''(0) = a - a^{-1}$, and, to order θ ,

$$X_P = -c\theta, \quad x_P = a^{-1}\theta, \quad z_P = -a. \quad (6.2)$$

If we linearize (2.10) in θ , we have

$$U_P = U - a\Lambda, \quad V_P = V + a^{-1}n\theta - a\Omega\theta. \quad (6.3)$$

Also $W = 0$ and $R = 1$ in this approximation, and equation (3.10)₃ implies that \dot{n} is also quadratic in small quantities; hence (in the linear approximation) we may take $n = \text{const.}$ (thus eliminating trivial perturbations which merely change n). Equations (3.7) and (3.10)_{1,2} then give

$$\left. \begin{aligned} \dot{U} - \dot{\varphi}V &= -\mu(U - a\dot{\theta}), \\ \dot{V} + \dot{\varphi}U &= -\mu\left(V - a\dot{\varphi}\theta + \frac{n\theta}{a}\right), \end{aligned} \right\} \quad (6.4)$$

and

$$\left. \begin{aligned} A(\ddot{\theta} - \dot{\varphi}^2\theta) + Cn\theta\dot{\varphi} &= c\theta + a\mu(U - a\dot{\theta}), \\ A(\ddot{\varphi}\theta + 2\dot{\varphi}\dot{\theta}) - Cn\dot{\theta} &= a\mu\left(V - a\dot{\varphi}\theta + \frac{n\theta}{a}\right). \end{aligned} \right\} \quad (6.5)$$

Now, as in Murakami (1995), let

$$\zeta = \theta e^{i\varphi}, \quad w = (U + iV)e^{i\varphi}. \quad (6.6)$$

Then

$$\dot{\zeta} = (\dot{\theta} + i\theta\dot{\varphi})e^{i\varphi}, \quad \ddot{\zeta} = ((\ddot{\theta} - \theta\dot{\varphi}^2) + i(\theta\ddot{\varphi} + 2\dot{\theta}\dot{\varphi}))e^{i\varphi}, \quad (6.7)$$

and

$$\dot{w} = ((\dot{U} + i\dot{V}) + i(U + iV)\dot{\varphi})e^{i\varphi}. \quad (6.8)$$

Hence (6.4) and (6.5) give

$$\dot{w} = -\mu w + a\mu\dot{\zeta} - i\mu a^{-1}n\zeta, \quad (6.9)$$

and

$$A\ddot{\zeta} - iCn\dot{\zeta} = (c + i\mu n)\zeta - \mu a^2\dot{\zeta} + \mu a w. \quad (6.10)$$

These equations admit solutions of the form

$$(\zeta, w) = (\hat{\zeta}, \hat{w})e^{pt}, \quad (6.11)$$

provided p satisfies a determinantal condition which reduces to the cubic equation

$$D_1(p; \mu) \equiv (p + \mu)(Ap^2 - iCnp - c) + \mu p(a^2p - in) = 0. \quad (6.12)$$

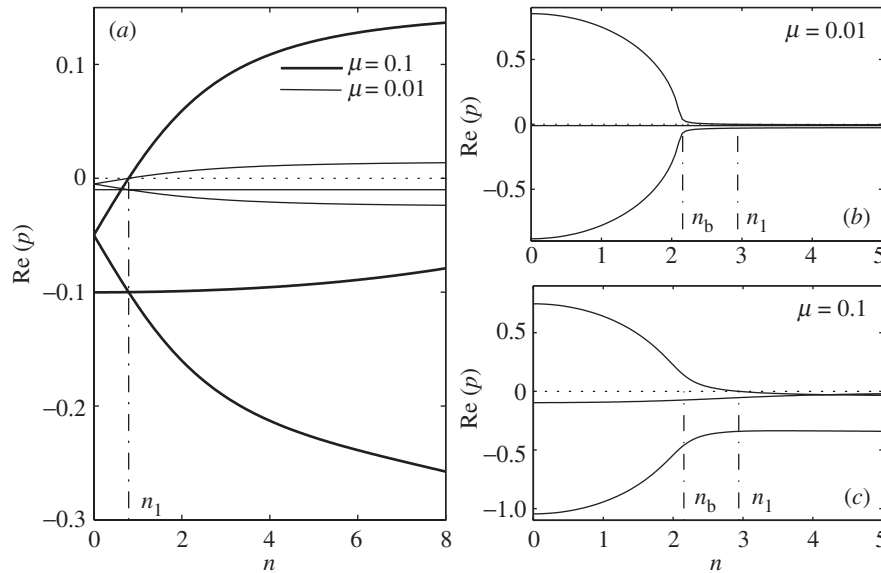


Figure 3. Real part of roots of (6.12) for a uniform spheroid for two values of the friction parameter μ : (a) oblate spheroid ($a = 0.5$), stable for $n < n_1$. (b), (c) Prolate spheroid ($a = 1.2$) subject to fast instability for $n < n_b$ and slow instability for $n_b < n < n_1$.

When $\mu = 0$, the roots of (6.12) are p_1, p_2, p_3 , where

$$p_1 = 0 \quad \text{and} \quad p_{2,3} = \frac{i(Cn \pm S)}{2A}, \quad (6.13)$$

with

$$S^2 = C^2 n^2 - 4Ac. \quad (6.14)$$

For stability with $\mu = 0$, we thus require that

$$n^2 > \frac{4Ac}{C^2}, \quad (6.15)$$

a condition that is always satisfied for an oblate spheroid ($c < 0$). For a prolate spheroid however, there is a bifurcation at

$$n = n_b = \frac{2\sqrt{Ac}}{C}. \quad (6.16)$$

For $n < n_b$, the orientation is unstable, the spin being insufficient to overcome the effect of gravity. We may describe this as a ‘fast’ instability[†], because its growth rate is $O(1)$ in the frictionless limit $\mu \rightarrow 0$ (this behaviour is evident in figure 3b, c).

Suppose now that $0 < \mu \ll 1$. Provided $S \neq 0$, the roots (6.13) are perturbed at order μ to

$$p_1 = -\mu \quad \text{and} \quad p_{2,3} = \frac{i(Cn \pm S)}{2A} - \frac{\mu(Sa^2 \pm n(a^2C - 2A))}{2AS}. \quad (6.17)$$

[†] This terminology is borrowed from dynamo theory, a ‘fast’ dynamo being one whose growth rate remains $O(1)$ as the magnetic resistivity tends to zero (see, for example, Childress & Gilbert 1995).

For stability of both oscillatory modes when $n > n_b$, we thus require in addition that

$$n^2(a^2C - 2A)^2 < a^4S^2, \quad (6.18)$$

which reduces to

$$(a^2C - A)n^2 > a^3(a^2 - 1). \quad (6.19)$$

Note that the condition $D > 0$ (see (5.17)) for the existence of intermediate states is also a necessary condition for the stability of vertical spin of a prolate spheroid, and also for the instability of spin with axis vertical of an oblate spheroid.

For the case of a uniform spheroid, $a^2C - A = \frac{1}{5}(a^2 - 1)$, and (6.19) becomes

$$n^2 \geq 5a^3 = n_1^2, \text{ say, according as } a \geq 1. \quad (6.20)$$

In this case,

$$n_b^2 = \frac{5(a^4 - 1)}{a} < n_1^2. \quad (6.21)$$

The uniform oblate spheroid thus becomes unstable at $\theta = 0$ if

$$n > n_1 = \sqrt{5a^3}. \quad (6.22)$$

The growth rate of this instability is $O(\mu)$ in the limit $\mu \rightarrow 0$; it is thus a ‘slow’ (or ‘secular’) instability. The uniform prolate spheroid by contrast is stable for $n > n_1$; for $n_b < n < n_1$, it is subject to a slow instability, and for $n < n_b$ it is subject to the fast instability already described.

These conclusions are illustrated in figure 3 which shows the three values of $\text{Re } p$ as a function of n for two typical cases: an oblate spheroid with $a = 0.5$ (figure 3*a*), for which $n_1 \approx 0.79$; and a prolate spheroid with $a = 1.2$ (figure 3*b, c*), for which $n_b \approx 2.11$, $n_1 \approx 2.94$. For both cases the roots are computed from the exact equation (6.12) for $\mu = 0.01$ and $\mu = 0.1$. In the prolate case, the distinction between the slow and fast regimes is very clear.

(b) *Stability of horizontal precession*

Consider now the linear stability of the steady state (5.13). Let $\theta = \frac{1}{2}\pi + \theta'$; linearizing in θ' then gives

$$x_P = -Z_P = 1, \quad X_P = (1 - a^{-2})z_P = (a^2 - 1)\theta'. \quad (6.23)$$

Since $n = 0$ in the undisturbed state, (3.12)₃ shows that $\dot{\Omega}$ is quadratic in small quantities; hence we may take $\Omega = \text{const}$. This reduces the dimension of the system from six to five (the neutrally stable mode corresponding to perturbation of Ω alone being suppressed). The linearized equations become

$$\left. \begin{aligned} \dot{U} - \Omega V &= -\mu(U - \dot{\theta}'), \\ \dot{V} + \Omega U &= -\mu(V + a^2\Omega\theta' + n), \\ A\ddot{\theta}' + A\Omega^2\theta' + Cn\Omega &= -(a^2 - 1)\theta' + \mu(U - \dot{\theta}'), \\ C\dot{n} &= -\mu(V + a^2\Omega\theta' + n). \end{aligned} \right\} \quad (6.24)$$

This fifth-order system admits solutions with $(U, V, \theta', n) \propto e^{pt}$, where p satisfies the determinantal condition

$$D_2(p; \mu) \equiv \begin{vmatrix} p + \mu & -\Omega & -\mu p & 0 \\ \Omega & p + \mu & \mu a^2 \Omega & \mu \\ -\mu & 0 & AG(p) + \mu p & C\Omega \\ 0 & \mu & \mu a^2 \Omega & Cp + \mu \end{vmatrix} = 0, \quad (6.25)$$

where

$$G(p) = F(p) + \frac{a^2 - 1}{A}, \quad F(p) = p^2 + \Omega^2. \quad (6.26)$$

By standard manipulations, this determinant may be written so that the parameter μ appears only in the first two rows. It is then evident that $D_2(p; \mu)$ is quadratic in μ : it reduces to

$$\begin{aligned} D_2(p; \mu) = & ACpG(p)F(p) \\ & + \mu\{AF(p)G(p) + C(p^2 - a^2\Omega^2)F(p) + 2ACp^2G(p)\} \\ & + \mu^2p(1 + C)(AG(p) + F(p)) = 0, \end{aligned} \quad (6.27)$$

a quintic equation for p . It is perhaps worth noting that $D_2(-p; -\mu) = -D_2(p; \mu)$.

When $\mu = 0$, the five roots of (6.27) are evidently

$$p_1 = 0, \quad p_{2,3} = \pm i\Omega, \quad p_{4,5} = \pm i \left(\Omega^2 + \frac{a^2 - 1}{A} \right)^{1/2}. \quad (6.28)$$

For prolate spheroids, the roots (6.28) all have zero real part and the corresponding fixed points are (linearly) neutrally stable. For oblate spheroids ($a < 1$), however, there is a bifurcation at

$$\Omega^2 = \Omega_b^2 = \frac{1 - a^2}{A}. \quad (6.29)$$

For $\Omega > \Omega_b$ the modes are all stable as for the prolate spheroid, but for $\Omega < \Omega_b$ the roots $p_{4,5}$ are real:

$$p_{4,5} = \mp (\Omega_b^2 - \Omega^2)^{1/2}, \quad (6.30)$$

and the mode corresponding to the root p_5 is unstable. This fast instability is of course again to be expected: the oblate spheroid set in spinning motion on its rim will fall over if the spin rate is insufficient to overcome the effect of gravity.

When $0 < \mu \ll 1$, the roots (6.28) are slightly perturbed, the perturbation being regular in the prolate case, but singular at the bifurcation point in the oblate case. It is expedient to consider these cases separately.

(i) *Prolate case* ($a > 1$)

Here we may consider a regular perturbation of each of the roots p_i ($i = 1, \dots, 5$) to order μ .

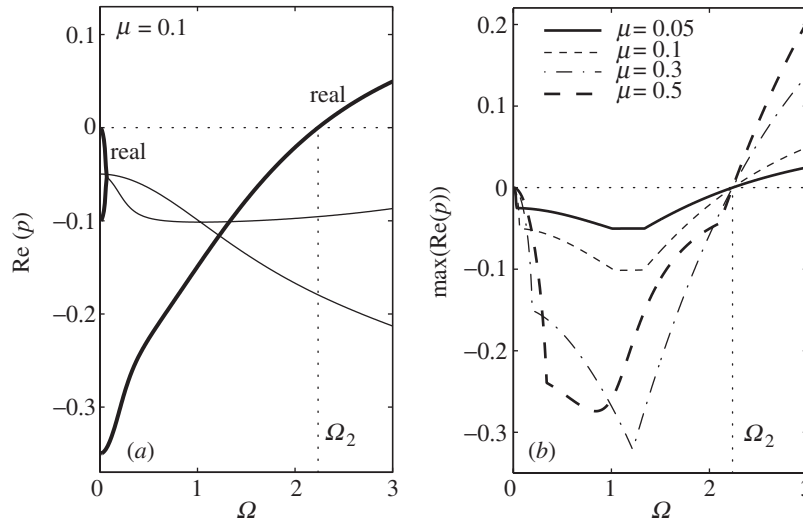


Figure 4. (a) Real parts of roots of (6.27) as a function of Ω for a uniform prolate spheroid with $a = 2$, $\mu = 0.1$; the real eigenvalues are as indicated in bold; (b) maximum real part as a function of Ω for $a = 2$ and four values of μ ; the instability threshold is always at $\Omega = \Omega_2 = \sqrt{5}$, a result associated with the viscous-friction model adopted for the stability analysis.

The root p_1 . This root is perturbed to $p_1 = \mu q$, say; substituting in (6.27) and retaining only terms of order μ , we obtain, for $\Omega \neq 0$,

$$q = \frac{\Omega^2(Ca^2 - A) - (a^2 - 1)}{C(A\Omega^2 + a^2 - 1)} = \frac{(Ca^2 - A)(\Omega^2 - D)}{AC(\Omega^2 + \Omega_1^2)}, \tag{6.31}$$

where

$$\Omega_1^2 = \frac{a^2 - 1}{A}, \quad D = \frac{a^2 - 1}{Ca^2 - A}. \tag{6.32}$$

Note that this is the same D as was encountered in (5.16). If $Ca^2 - A < 0$ (as, for example, for the polar spheroid (5.4)), then $q < 0$, i.e. the mode is damped by friction. If, however, $Ca^2 - A > 0$ (as, for example, for the uniform spheroid (5.3) or the equatorial spheroid (5.5)), then $D > 0$; q is then positive for

$$\Omega^2 > D = \Omega_2^2, \text{ say.} \tag{6.33}$$

The corresponding mode is then subject to slow instability with growth rate μq . Note that here the condition $D > 0$ for the existence of intermediate states now appears as a necessary condition for instability in the prolate case. For the important case of a uniform spheroid,

$$\Omega_1^2 = \frac{5(a^2 - 1)}{a^2 + 1}, \quad \Omega_2^2 = 5, \quad q = \frac{1}{2}\Omega_1^2 \frac{\Omega^2 - 5}{\Omega^2 + \Omega_1^2}, \tag{6.34}$$

and we have a slow instability for

$$\Omega^2 > 5. \tag{6.35}$$

We may seek to understand this instability as follows. In the unstable mode with $\mu \ll 1$, we have

$$\dot{\theta}' = O(\mu), \quad \ddot{\theta}' = O(\mu^2). \tag{6.36}$$

Moreover, from (6.24)₃, $U = O(\mu)$ and $V = O(\mu^2)$, and the primary balance in (6.24) is

$$A\Omega^2\theta' + Cn\Omega = -(a^2 - 1)\theta'. \quad (6.37)$$

Thus, θ' is related to n in quasi-static manner. At leading order in μ , the slip velocity is $\mathbf{U}_P = V_P\mathbf{j}$, where

$$V_P = a^2\Omega\theta' + n = \left[1 - \frac{a^2C\Omega^2}{A\Omega^2 + a^2 - 1}\right]n, \quad (6.38)$$

and (6.24)₄ gives, at the same leading order

$$\dot{n} = \mu q n, \quad (6.39)$$

where q is as given by (6.31). The source of the instability is thus evident in the torque exerted by the frictional force $\mathbf{F} \approx -\mu V_P\mathbf{j}$, which tends to increase the spin n , the feedback being positive when the condition (6.33) is satisfied.

The situation is further simplified when

$$A\Omega^2 \gg (a^2 - 1). \quad (6.40)$$

Then (6.37) becomes

$$A\Omega\theta' + Cn \approx 0. \quad (6.41)$$

Here we recognize the gyroscopic approximation (4.1) for θ near $\pi/2$. Thus it is evident that, when $\mu \ll 1$ and (6.40) is also satisfied, the mode of secular instability that is realized is indeed governed by the gyroscopic approximation. (It was in fact through such consideration that we first recognized the possibility of extending the gyroscopic approximation into the nonlinear regime, as described in MS02.)

The roots $p_{2,3} = \pm i\Omega$. These are similarly perturbed to, say, $p = \pm i\Omega + \mu q$. Since $F(\pm i\Omega) = 0$, we have $F(p) \approx \mu q F'(\pm i\Omega) = \pm 2\mu q i\Omega$. Hence (6.27) easily gives

$$p_{2,3} = \pm i\Omega - \mu, \quad (6.42)$$

i.e. both modes are damped by the frictional effect.

The roots $p_{4,5} = \pm i(\Omega^2 + (a^2 - 1)/A)^{1/2}$. We write similarly $p = p_{4,5} + \mu q$. In this case,

$$G(p_{4,5}) = 0, \quad G(p) \approx \mu q G'(p_{4,5}) = 2\mu q p_{4,5}, \quad F(p_{4,5}) = -\frac{a^2 - 1}{A},$$

and (6.27) gives

$$q = -\frac{1}{2A} \left(1 + \frac{a^2\Omega^2}{\Omega^2 + \Omega_1^2}\right). \quad (6.43)$$

This is real and negative, and so these modes are also damped by the frictional effect, whatever the value of Ω .

To summarize, for a prolate spheroid for which $Ca^2 - A > 0$, there is one non-oscillatory unstable mode when the condition (6.33) is satisfied. When Ω^2 is sufficiently above this threshold for instability, its structure is governed by the gyroscopic

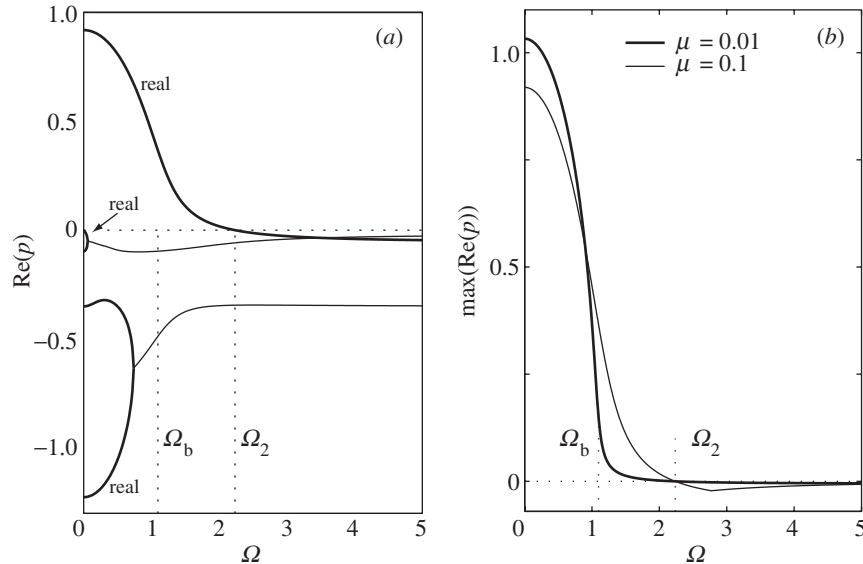


Figure 5. (a) Real parts of roots of (6.27) as a function of Ω for an oblate spheroid with $a = 0.8$ and $\mu = 0.1$; real eigenvalues are indicated in bold type; (b) maximum real part as a function of Ω for $\mu = 0.01$ and $\mu = 0.1$. Note the slow instability for $\Omega_b < \Omega < \Omega_2$ and the fast instability for $\Omega < \Omega_b$.

balance condition (6.41). There are also four oscillatory modes (two complex conjugate pairs) which are all damped by friction in the linear stability analysis. In the terminology of dynamical systems (see, for example, Guckenheimer & Holmes 1983), the unstable manifold is one dimensional (two dimensional if the unstable manifold emerging from the *line* of non-isolated fixed points ($\theta = \pi/2, n = 0$) is considered). The results are confirmed by numerical determination of the roots of (6.27). Figure 4a shows the real parts of the roots (one real, two complex conjugate) for a uniform spheroid with $a = 2$, $\mu = 0.1$ as a function of Ω . The onset of instability at $\Omega = \Omega_2 = \sqrt{5}$ is evident, consistent with the fact that for a uniform spheroid, from (6.27), $D_2(0, \mu) = \mu\Omega^2(a^2 - 1)(1 - \Omega^2/5)$. Figure 4b shows the maximum of these real parts for various values of μ ; for the uniform spheroid and with viscous friction, there is evidently no instability for $\Omega < \sqrt{5}$, even for the larger values of μ .

(ii) *Oblate case* ($a < 1$)

For this case, the above type of perturbation analysis may be carried out provided Ω is not near the bifurcation point $\Omega = \Omega_b$ (given by (6.29)). We simply summarize the results for the case of a uniform oblate spheroid for which

$$\Omega_2^2 = 5, \quad \Omega_b^2 = \frac{5(1 - a^2)}{1 + a^2} < \Omega_2^2. \quad (6.44)$$

For $\Omega > \Omega_2$ the state $\theta = \pi/2$ is stable. For $\Omega_b < \Omega < \Omega_2$, it is subject to slow instability; and for $\Omega < \Omega_b$, it is subject to fast instability.

This behaviour is shown in figure 5 for a uniform oblate spheroid with $a = 0.8$; for this case $\Omega_2^2 = 5$, $\Omega_b^2 \approx 1.1$. Figure 5a shows the real parts of p as a function of

Ω for $\mu = 0.1$, while figure 5*b* shows the maximum of these values for $\mu = 0.01$ and $\mu = 0.1$. In the former case, the regime of slow instability ($\sqrt{1.1} < \Omega < \sqrt{5}$) is quite evident.

(c) *Stability of intermediate states*

We shall suppose in this subsection that the condition $D > 0$ (or equivalently, (5.17)) for the existence of intermediate steady states is satisfied. In any such state, $U = V = A = 0$ and (Ω, n, θ) are related by (5.14), (5.15). Let $\Xi_0 = (0, 0, \Omega_0, 0, \theta_0, n_0)$ represent one such state, and suppose this to be perturbed to

$$\Xi = \Xi_0 + \Xi'. \quad (6.45)$$

The corresponding linearization of $\dot{\Xi} = \mathcal{F}(\Xi)$ is of the form

$$\dot{\Xi}' = M_0 \Xi', \quad (6.46)$$

where M_0 is the matrix $\mathcal{F}'(\Xi_0)$. This equation has solutions of the form $\Xi' = \hat{\Xi} e^{pt}$, where p satisfies a determinantal condition which reduces to the polynomial equation

$$pD_3(p; \mu) \equiv p(p^5 + c_4 p^4 + c_3 p^3 + c_2 p^2 + c_1 p + c_0) = 0. \quad (6.47)$$

The coefficients c_0, \dots, c_4 , obtained with the help of MAPLE, are given in the appendix. Note that c_1, c_3 are even, and c_0, c_2, c_4 odd (actually linear) in μ . Thus, again in this case, D_3 satisfies the symmetry condition $D_3(-p; -\mu) = -D_3(p; \mu)$. The expressions for c_0, \dots, c_4 involve a parameter α given by

$$\alpha = (\lambda - 2)^2 \cos^2 \theta_0 + \sin^2 \theta_0 \frac{(a^2 - 1) \cos^2 \theta_0 + \lambda}{(a^2 - 1) \cos^2 \theta_0 + 1}, \quad (6.48)$$

where $\lambda = a^2 C/A$. As shown in the appendix, $\alpha > 0$ for both prolate and oblate spheroids.

The factor p in (6.47) is to be expected: it corresponds to neutrally stable perturbations in phase-space in the direction tangent to the continuous curve of intermediate states (figure 2). The corresponding eigenvector thus depends on θ_0 . We may disregard such perturbations in what follows.

Consider first the situation when $\mu = 0$. Then (6.47) gives

$$D_3(p; 0) = p(p^4 + d_3 p^2 + d_1) = 0, \quad (6.49)$$

where

$$d_3 = c_3|_{\mu=0} = \frac{A\Omega_0^2(\alpha + 1 + X_{P0}^2/A)}{A + X_{P0}^2}, \quad d_1 = c_1|_{\mu=0} = \frac{A\Omega_0^4\alpha}{A + X_{P0}^2}. \quad (6.50)$$

The roots are

$$p_1^{(0)} = 0, \quad p_{2,3}^{(0)} = \pm i\Omega_0, \quad p_{4,5}^{(0)} = \pm i\Omega_0 \left(\frac{A\alpha}{A + X_{P0}^2} \right)^{1/2}. \quad (6.51)$$

Since $\text{Re } p_j^{(0)} = 0$ ($j = 1, \dots, 5$), the state Ξ_0 is (linearly) neutrally stable when $\mu = 0$.

Note that if

$$A\alpha = A + X_{P0}^2, \quad (6.52)$$

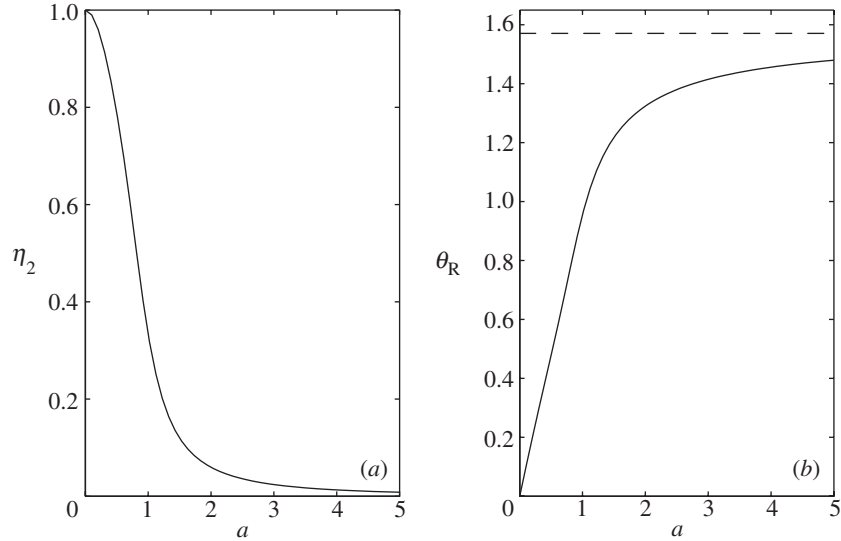


Figure 6. The positive root η_2 of (6.53) as a function of a , and the corresponding variation of the angle θ_R of resonant instability.

then there is a resonance between the $p_{2,3}^{(0)}$ modes and the $p_{4,5}^{(0)}$ modes. Equation (6.52) is a quadratic equation for $\eta = \cos^2 \theta_0$, and this resonance occurs only if this quadratic has a real root between 0 and 1. For the case of a uniform spheroid, the quadratic equation reduces to

$$2(a^2 - 1)(2a^2 + 1)\eta^2 - (5a^4 + 2a^2 - 1)\eta + (a^2 + 1) = 0, \quad (6.53)$$

and this does indeed have a real root between 0 and 1 for all values of a (see figure 6). The resonance does therefore always exist in this case at an angle θ_R , say, dependent on a . (The situation is a little more complicated for the cases of polar and equatorial spheroids.)

Provided we are not too near this resonant angle, it is to be expected that when $0 < \mu \ll 1$, the roots will be slightly perturbed to

$$p_j = i\xi_j + \mu q_j, \quad (6.54)$$

where $i\xi_j = p_j^{(0)}$. Substitution into (6.47) and retaining only terms linear in μ gives

$$q_j = \frac{-c_4 \xi_j^4 + c_2 \xi_j^2 - c_0}{\mu(5\xi_j^4 - 3d_3 \xi_j^2 + d_1)}. \quad (6.55)$$

These values of q_j do not depend on μ because of the linearity of c_0 , c_2 and c_4 in μ noted above. Using these expressions, the five perturbed roots are found in the form

$$p_1 = -\mu x_{P0} \left(\frac{x_{P0}}{C} - \frac{a^2 \beta}{A\alpha} \right), \quad p_{2,3} = \pm i\Omega_0 - \mu, \quad (6.56)$$

and

$$p_{4,5} = p_{4,5}^{(0)} - \frac{\mu}{2} \left(\frac{a^2 x_{P0}}{A\alpha} (\beta - \alpha z_{P0} \cot \theta_0) + \frac{Z_{P0}^2}{A + X_{P0}^2} \right), \quad (6.57)$$

where β is also as given in the appendix. At least for the case of a uniform spheroid, $q_j < 0$ for each j , so that friction is stabilizing at $O(\mu)$.

Figure 7*a* shows computed values of $\text{Re}(p_j)$ as a function of θ_0 based on the exact equation (6.48), for $\mu = 0.1$ and two values of a ($a = 0.5$ for which $\theta_R \approx 0.48$, and $a = 2$ for which $\theta_R \approx 1.32$). The effect of the resonances is evident for both cases; this effect is not captured in the $O(\mu)$ analysis above: it is a higher-order effect which is nevertheless important because it indicates a very small (actually $O(\mu)$) region of instability in the neighbourhood of the resonant angle, in which $\text{Re} p_{4,5}$ is positive (and also $O(\mu)$). Parts (b) and (c) of figure 7 show the maximum of the real parts of p_j for various values of a and μ , respectively. The unstable band becomes increasingly spiked as μ decreases towards zero. However, the magnitude of the positive real part in the unstable band remains small compared with the magnitudes of the (negative) real parts of the other eigenvalues which correspond to stable disturbances (figure 7*a*). Trajectories near the resonant angle are in fact rapidly attracted towards the fixed-point line and then slowly shifted along the line to fixed points outside the unstable band (see figure 9).

(d) *Stability of pure rolling states*

Finally, consider a pure rolling state, for which $\Xi_0 = (0, V_0, 0, 0, \frac{1}{2}\pi, n_0)$, with $V_0 = -n_0$, and again, let $\Xi = \Xi_0 + \hat{\Xi}e^{pt}$. In this case, linearization of the system (3.12) leads to

$$p^2 D_4(p; \mu) \equiv p^2 [Cp^2 Q(p) + \mu p \{(1 + 2C)Q(p) + ACp^2 + C^2 n_0^2\} + \mu^2 (1 + C) \{Ap^2 + n_0^2 C + Q(p)\}] = 0, \quad (6.58)$$

where

$$Q(p) = A^2 p^2 + A(a^2 - 1) + C^2 n_0^2. \quad (6.59)$$

Here, there is a *double* root $p_{0,1} = 0$. The corresponding linearly independent eigenvectors are

$$\hat{\Xi}_0 = (0, -1, 0, 0, 0, 1), \quad \hat{\Xi}_1 = (-n_0, 0, \mu, 0, \mu n_0 (C + 1)(a^2 - 1)^{-1}, 0). \quad (6.60)$$

The first of these corresponds to neutrally stable perturbations along the line (in phase space) of pure rolling states. The second corresponds to perturbations in a direction orthogonal to this line; it is neutrally stable only in linear analysis. Centre-manifold analysis using the basis vectors (6.60) shows that, under general perturbation, the rolling states are weakly unstable due to nonlinear effects. Trajectories computed with a starting point near pure rolling states are consistent with this conclusion: these lead—at any rate for the prolate spheroid—from the (unstable) rolling state (for which the angular momentum \mathbf{H} is horizontal) to a precessional or intermediate state (for which \mathbf{H} is vertical or oblique).

Turning now to the roots of the quartic $D_4(p; \mu) = 0$, when $\mu = 0$ these are

$$p_{2,3}^{(0)} = 0, \quad p_{4,5}^{(0)} = \pm \frac{i(A(a^2 - 1) + C^2 n_0^2)^{1/2}}{A}. \quad (6.61)$$

Again for the oblate case ($a < 1$), there is a fast instability if

$$n_0^2 < \frac{A(1 - a^2)}{C^2} = n_2^2. \quad (6.62)$$

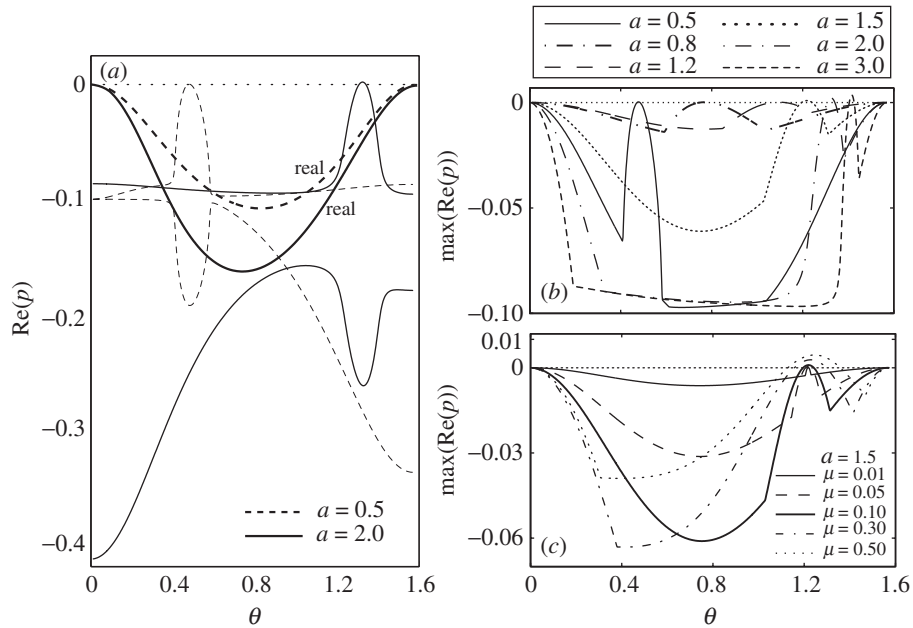


Figure 7. Stability of the intermediate states: (a) real parts of the roots of (6.47) as a function of the inclination angle θ of the steady state; real eigenvalues are as indicated. (b) Maximum real part of the five eigenvalues along the fixed-point curve parametrized by θ . (c) Similar to (b) but with a fixed and μ varied.

Provided we are not near this bifurcation point, when $0 < \mu \ll 1$ the roots may be obtained by the now familiar procedure, giving, to $O(\mu)$,

$$p_2 = -\frac{\mu(1+C)}{C}, \quad p_3 = -\mu \left(1 + \frac{Cn_0^2}{A(a^2-1) + C^2n_0^2} \right), \quad (6.63)$$

and

$$p_{4,5} = p_{4,5}^{(0)} + \mu q, \quad \text{where } q = \frac{C(A-C)n_0^2 - A(a^2-1)}{2A(A(a^2-1) + C^2n_0^2)}. \quad (6.64)$$

If $q > 0$, then we have slow instability.

For the case of a uniform spheroid, (6.64) reduces to

$$q = \frac{5(a^2-1)(2n_0^2 - 5(a^2+1))}{2(a^2+1)(4n_0^2 + 5(a^4-1))}. \quad (6.65)$$

Thus, for a prolate spheroid rolling on a plane with its axis horizontal, we have slow instability if

$$n_0^2 > \frac{5}{2}(a^2+1) = n_3^2. \quad (6.66)$$

This instability may or may not dominate over the nonlinear instability referred to above, depending on the amplitude of the initial disturbance from the steady state.

Similarly, a uniform oblate spheroid ($a < 1$) is subject to a slow instability for

$$n_0^2 < \frac{5}{2}(a^2+1). \quad (6.67)$$

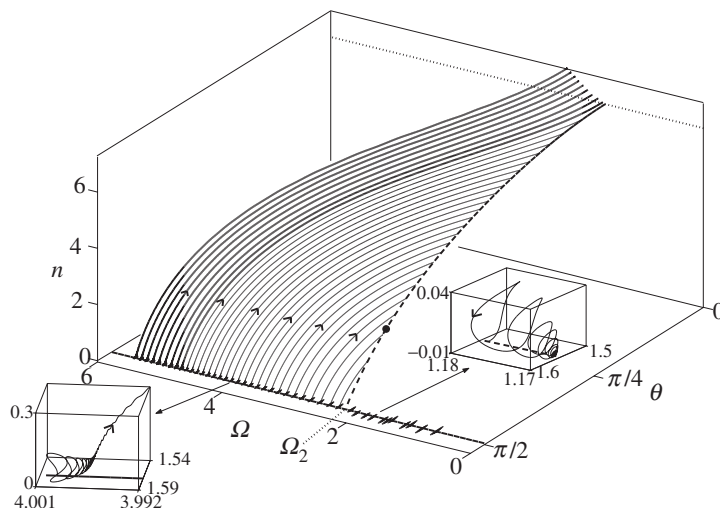


Figure 8. Trajectories of the system (3.12) projected onto the subspace of the variables (Ω, θ, n) for a uniform prolate spheroid ($a = 2$), with viscous friction ($\mu = 0.1$). The dashed curve is that of intermediate steady states (5.14), (5.15). The small bullet point indicates the centre of the unstable band around the resonant angle θ_R . For $\Omega_0 > \Omega_2 = \sqrt{5}$, fixed points on $\theta = \pi/2$ are unstable, and the trajectories are attracted to stable fixed points either on the dashed curve or (for $\Omega_0 > \Omega_V \approx 5.06$) on the plane $\theta = 0$ above the dotted line ($n = \sqrt{5}a^3 \approx 6.32$). The two insets show blow-ups of trajectories near two fixed points (one stable, one unstable) on $\theta = \pi/2$.

Just as for the stability of horizontal precession (figure 5), this slow instability is triggered by friction over a range of values of n_0 ($n_2 < n_0 < n_3$) greater than the value n_2 (equation (6.62)) at which the fast instability sets in.

7. Numerical treatment

We now present the results of some computations based on the exact system (3.12). We used an adaptive method based on second-order numerical differentiation formulae due to Klopfenstein (1971) and similar to that described by Shampine (1980). This method has two desirable properties: easy implementation of time-step adaptivity and allowance for possible stiffness of the system (associated with L-stability). For most runs, we used a relative error tolerance 10^{-9} .

(a) System trajectories

We focus here on the case of a uniform prolate spheroid with $a = 2$, and with viscous friction at the point P. The trajectories lie in the six-dimensional phase space; here we show simply their projections in the three-dimensional subspace of the variables (Ω, θ, n) . Figure 8 shows a number of trajectories starting from initial conditions ($U = 0, V = 0, \Omega_0, \Lambda = 0.01, \theta = \pi/2, n = 0$). It is evident that the points with $\Omega_0 \leq \sqrt{5}$ are stable whereas those for which $\Omega_0 > \sqrt{5}$ are unstable. Trajectories originating near the unstable fixed points are attracted along the unstable manifold either to one of the intermediate-state fixed-points at an angle $\theta_F > 0$ or, if Ω_0 is sufficiently large (greater than Ω_V , say), to a fixed point for which $\theta_F = 0$ and $n = n_F$, say; in this case, the spheroid rises fully to a stable vertical position. The

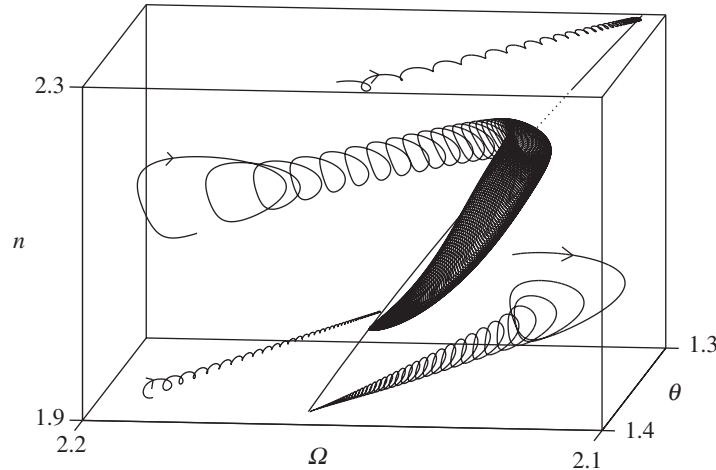


Figure 9. Blow-up of four trajectories in the vicinity of the bullet point of figure 8. The band of unstable fixed points is shown dotted; the trajectory that spirals in towards this band then slowly drifts to a stable fixed point outside the band.

blow-ups in the insets show damped oscillations in the immediate neighbourhood of the fixed points; these depend on the precise initial conditions adopted, and are to be expected in view of the existence of the damped oscillatory modes identified in the foregoing stability analysis.

For $a = 2$ the resonant instability discussed in § 6 *c* above occurs at $\theta = \theta_R \approx 1.32$ (see figure 6); this is marked by the bullet on the dashed curve of figure 8. Close examination of the trajectories near this point (figure 9) shows rapid attraction towards the dashed curve coupled with slow drift to points outside the narrow band of resonant instability.

Similar computations using Coulomb (rather than viscous) friction (for which the set of fixed points is unchanged) give similar trajectories except very near the fixed points, where Coulomb friction becomes indeterminate in direction (and therefore of dubious validity) and where the trajectories exhibit oscillations suggestive of limit-cycle behaviour (shown later in figure 12*b*).

The second critical angular velocity Ω_V above which a uniform prolate spheroid will rise to the vertical may be estimated using the gyroscopic approximation discussed in § 4; for then we have Jellett's constant which gives

$$n_F a = \frac{\Omega_0 A}{C} = \frac{1}{2}(1 + a^2)\Omega_0. \quad (7.1)$$

From (6.22), this spin is stable provided $n_F > \sqrt{5a^3}$; hence the condition that the spheroid rises to a vertical state that is *just* stable implies that

$$\Omega_V^2 = \frac{20a^5}{(1 + a^2)^2}, \quad > 5 \text{ for } a > 1. \quad (7.2)$$

Figure 10 shows the asymptotic angle of inclination θ_F as a function of the initial rate of precession Ω_0 for various values of $a > 1$. The critical value Ω_V is where these curves hit the axis $\theta_F = 0$. The inset figure shows this Ω_V as a function of a , showing agreement to within about 5% with the above formula (7.2). This indicates

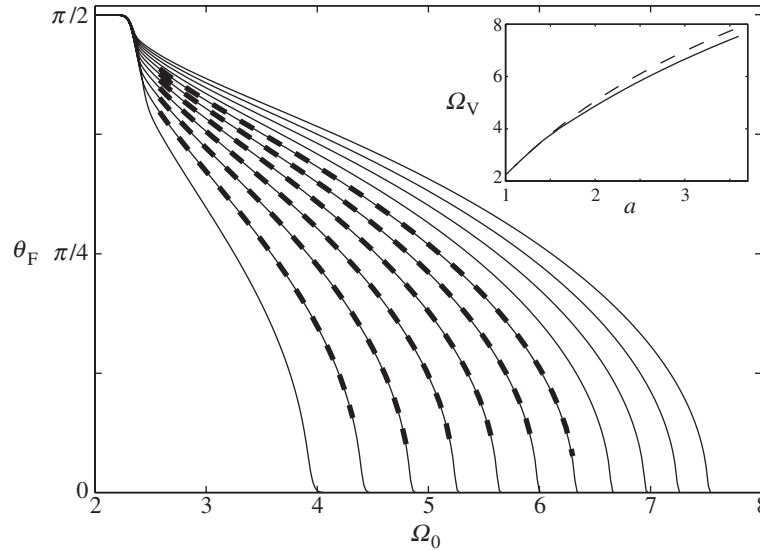


Figure 10. Final (asymptotic) value θ_F as a function of the initial precessional angular velocity Ω_0 , for a trajectory originating near a fixed-point ($\Omega_0, \theta = \pi/2, n = 0$), for various values of a (left to right, $a = 1.6, 1.8, 2.0, 2.2, 2.4, 2.6, 2.8, 3.0, 3.2, 3.4, 3.6$) and for $\mu = 0.1$ (thin solid) and $\mu = 0.2$ (thick dashed). The curves hit the axis $\theta_F = 0$ at $\Omega_0 = \Omega_V$, and the inset shows the variation (solid curve) of this Ω_V as a function of a ; this compares quite well with the estimate (7.2) based on the gyroscopic approximation (dashed curve).

that even when the precessional speed is only just sufficient to raise the axis to the vertical, the gyroscopic approximation works reasonably well. Note that figure 10 is insensitive to change of μ ; indeed the curves (thick dashed) obtained with $\mu = 0.2$ are indistinguishable from those (thin solid) for $\mu = 0.1$. The evidence here is that, at least within the parameter range of these computations, the value of μ affects the time taken to follow a trajectory in phase-space, but not its final destination.

(b) Validity of the gyroscopic approximation

The linear stability analysis of §6 indicates that when μ is small, $\Lambda = \dot{\theta}$ is $O(\mu)$ during the linear phase of evolution along the unstable manifold. As shown by MS02, under the gyroscopic approximation this behaviour persists during the subsequent nonlinear evolution also. Figure 11 shows the evolution of Λ for the rise of a prolate spheroid for several values of Ω_0 and for two values of μ (0.01 and 0.1). In both cases it is evident that Λ does indeed remain of the order of μ . (The curves for $\Omega_0 = 15$ show oscillations of such high frequency that they appear blurred, although in fact they are well resolved; we are confident that they are not numerical artefacts.) These oscillations induce corresponding oscillations in R via (3.14), and are a prelude to the jumping phenomenon referred to in the introduction; analysis of this phenomenon is deferred to part II.

Figure 12a shows the computed time evolution of the angle θ from unstable to stable states for an oblate ($a = 0.5$) and a prolate ($a = 2$) spheroid. In both cases, the curves closely shadow the thick solid curves, previously obtained by MS02 under the gyroscopic approximation. The oscillations are interesting; these are filtered out

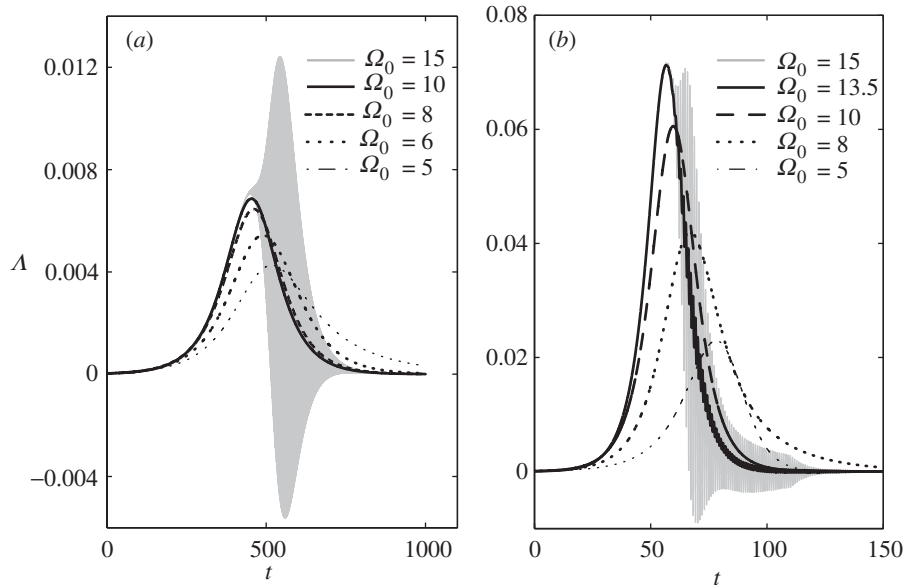


Figure 11. Time evolution of $A = \dot{\theta}$ during the rise of a prolate spheroid ($a = 2$) for various Ω_0 : (a) $\mu = 0.01$; (b) $\mu = 0.1$. In both cases A remains $O(\mu)$. The rapid oscillations that appear with increasing Ω_0 (here with amplitude $O(\mu)$) lead to corresponding oscillations in R , and are a prelude to the jumping phenomenon.

in the gyroscopic approximation, just as inertial waves are filtered out under the geostrophic approximation in geophysical fluid dynamics. Figure 12*b* shows similar evolution when Coulomb (rather than viscous) friction is used.

The gyroscopic approximation leads to the gyroscopic balance condition (4.1). Figure 13*a* shows the evolution of Cn and $A\Omega \cos \theta$ separately, and also of their difference $G = |Cn - A\Omega \cos \theta|$ for $\Omega_0 = 10$. It is evident that for this value, gyroscopic balance is achieved to within about 5%. This balance improves as Ω_0 increases, but the incidence of strong oscillations eventually invalidates the gyroscopic approximation. Figure 13*b* shows the extent to which the Jellett ‘constant’ remains constant for different values of Ω_0 ; note again that, for $\Omega_0 = 10$, the variation is within 5%. Figure 13*c, d* shows the evolution of G with time for various values of Ω_0 and $a (> 1)$; gyroscopic balance improves as either Ω_0 increases or $(a - 1)$ decreases.

8. Discussion and conclusions

Despite the apparent simplicity of the problem addressed in this paper, the detailed analysis has revealed a remarkable richness of structure in dynamical behaviour. The governing nonlinear dynamical system is six-dimensional and, even for the prototype problem of a uniform spheroid under viscous friction at the point P, there remain two independent parameters (a and μ), so that a complete exploration of all possible behaviours in the six-dimensional phase-space is a formidable undertaking.

A framework is, however, provided by a classification of the fixed points (or steady states) of the system, and analysis of the stability of these fixed points under small perturbations. This analysis, presented in §§ 5 and 6, provides a guide map to the choice of computed trajectories of the system, as presented in § 7. A guiding theme

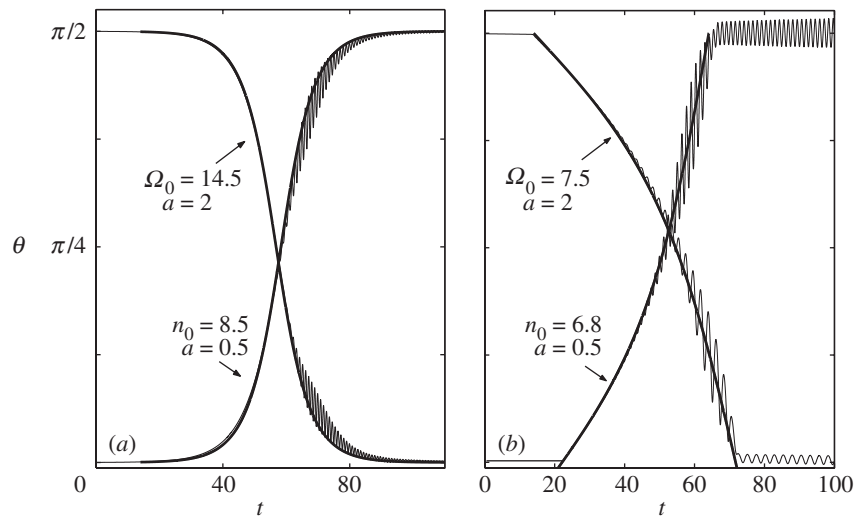


Figure 12. (a) Evolution of θ under viscous friction ($\mu = 0.1$) from unstable to stable equilibrium for a prolate ($a = 2$) and an oblate ($a = 0.5$) spheroid; the thick solid curves denote solutions under the gyroscopic approximation. (b) The same under Coulomb friction with $\mu = 0.1$.

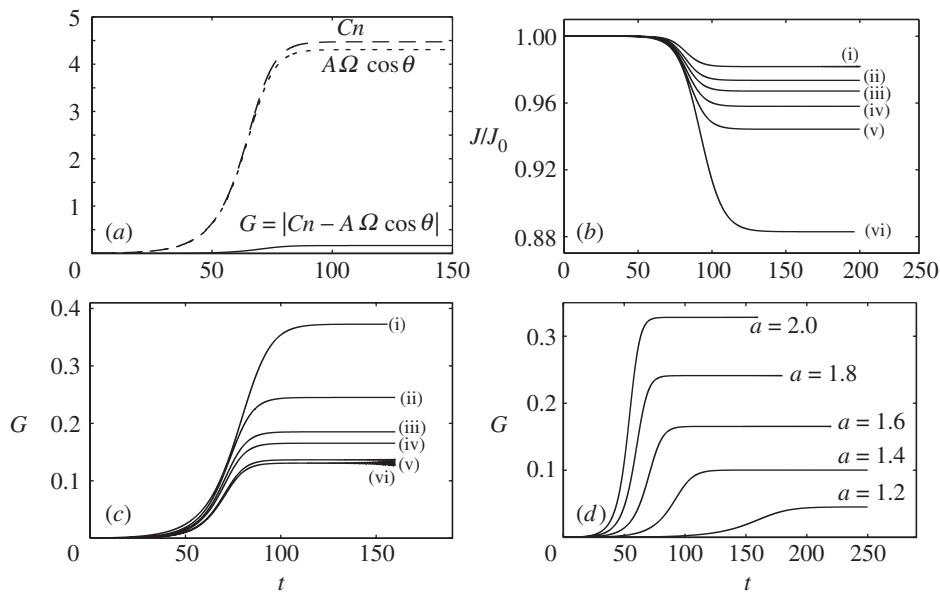


Figure 13. (a) Evolution of Cn , $A\Omega \cos \theta$ and $G = |Cn - A\Omega \cos \theta|$ during the rise of a uniform prolate spheroid; $\Omega_0 = 10$, $a = 1.6$, $\mu = 0.1$. (b) Evolution of the normalized Jellett 'constant' measured on trajectories originating near fixed points ($\Omega_0, \theta = \pi/2, n = 0$); $a = 1.6$, $\mu = 0.1$; (i) $\Omega_0 = 12$; (ii) $\Omega_0 = 10$; (iii) $\Omega_0 = 9$; (iv) $\Omega_0 = 8$; (v) $\Omega_0 = 7$; (vi) $\Omega_0 = 5$. (c) Evolution of G for $a = 1.6$, $\mu = 0.1$ and various Ω_0 ; (i) $\Omega_0 = 5$; (ii) $\Omega_0 = 7$; (iii) $\Omega_0 = 9$; (iv) $\Omega_0 = 10$; (v) $\Omega_0 = 12$; (vi) $\Omega_0 = 12.5$. (d) the same for $\Omega_0 = 10$, $\mu = 0.1$ and various a .

has been the concept of gyroscopic balance, as previously introduced by MS02, which applies when friction is weak and the Coriolis force is dominant, and which in effect provides a one-dimensional description of the dynamics, from which any latent oscillatory modes of motion have been filtered out. The numerical work of § 7 has allowed a partial assessment of the usefulness of this greatly simplified description.

We have restricted attention to circumstances in which the normal reaction R at P remains positive. However, we note that when the initial angular momentum imparted to the spheroid is sufficiently large, the growth of oscillatory modes can be such as to reduce R to zero, in which case the spheroid may lose contact with the table. This ‘jumping’ phenomenon is the subject of a further paper in preparation (part II).

We have emphasized the distinction between ‘fast’ and ‘slow’ modes of instability, the fast modes being those that survive in the limit $\mu \rightarrow 0$. This distinction helps in understanding the structure of the growth rate (instability) diagrams presented in figures 3 and 5. The (slow) resonant instability encountered in § 6 *c* is intriguing, and perhaps merits further investigation. It is reminiscent of the ‘elliptic’ instability that occurs in two-dimensional fluid flows with elliptic streamlines (see, for example, Saffman 1992, § 12.4).

Further generalizations are clearly possible: spheroids with displaced centre-of-mass ($d \neq 0$), axisymmetric bodies of non-spheroidal shape including those that are not everywhere convex, even spheroids with internal fluid-filled cavities. It is hoped to address such generalizations in future communications.

H.K.M. acknowledges the support of the Fondation de l’Ecole Normale Supérieure, Paris, through his tenure of the Chaire Internationale de Recherche Blaise Pascal (2001–2003). Y.S. thanks the Hopkinson and the Computational Fluid Dynamics laboratories of the Department of Engineering, University of Cambridge, for providing research facilities during a period of leave in the UK. This work is partly supported by the Daiwa Anglo-Japanese Foundation, the Trinity College Visiting Scholars Fund and the Keio Gijyuku Academic Development Fund. M.B. is supported by a scholarship of the Gates Cambridge Trust.

Appendix A.

The coefficients, c_4, \dots, c_0 , of the characteristic polynomial $D_3(p, \mu)$ (equation (6.47)) obtained in § 6 *c* are, with $h_0 = h(\theta_0)$, $h'_0 = h'(\theta_0)$:

$$\begin{aligned}
 c_4 &= \mu \left(2 + \frac{x_{P0}^2}{C} + \frac{h_0^2}{A + h_0'^2} - a^2 x_{P0} z_{P0} \frac{\cot \theta_0}{A} \right), \\
 c_3 &= \frac{1}{A + h_0'^2} \left\{ A \Omega_0^2 \left(\alpha + 1 + \frac{h_0'^2}{A} \right) \right. \\
 &\quad \left. + \left(\frac{\mu^2}{AC h_0'^2} \right) (h_0^2 + A + h_0'^2) \{ a^2 (a^2 C - A) \cos^2 \theta_0 + A(1 + C) h_0'^2 \} \right\}, \\
 c_2 &= \frac{\mu A \Omega_0^2}{A + h_0'^2} \left\{ \frac{x_{P0}^2 (\alpha + 1 + h_0'^2/A)}{C} + \frac{h_0^2}{A} + 2\alpha \right. \\
 &\quad \left. - a^2 x_{P0} \frac{\beta + z_{P0} (1 + h_0'^2/A) \cot \theta_0}{A} \right\},
 \end{aligned}$$

$$c_1 = \frac{1}{A + h_0^2} \left\{ A\Omega_0^4 \alpha + \left(\frac{\mu^2 \Omega_0^2}{AC h_0^4} \right) \left\{ -A(h_0^2 - 1)(a^2 C - A) \sin^4 \theta_0 \right. \right. \\ \left. \left. + [(a^2 C - A)((a^2 C(a^2 + 2) - 4A)h_0^2 + Ca^4) \cos^2 \theta_0 \right. \right. \\ \left. \left. + h_0^2(((A + a^2 + 1)C + 1)h_0^2 + C(a^2 C - A))A] \sin^2 \theta_0 \right. \right. \\ \left. \left. + h_0^4 C \cos^2 \theta_0 (a^2(C - 1) - 2A)^2 \right\} \right\} \\ c_0 = \frac{\mu A \Omega_0^4}{A + h_0^2} \left(\frac{x_{P0} \alpha}{C} - \frac{a^2 \beta}{A} \right) x_{P0},$$

where x_{P0} , z_{P0} are given by (2.16) at $\theta = \theta_0$, and α and β are given by

$$\alpha = (\lambda - 2)^2 \cos^2 \theta_0 + \sin^2 \theta_0 \frac{(a^2 - 1) \cos^2 \theta_0 + \lambda}{(a^2 - 1) \cos^2 \theta_0 + 1}, \quad (\text{A } 1)$$

$$\beta = x_{P0} (1 - (\lambda - 1) \cos^2 \theta_0) + (\lambda - 1) \left(1 + \frac{1}{h_0^2} \right) z_{P0} \sin \theta_0 \cos \theta_0, \quad (\text{A } 2)$$

with $\lambda = a^2 C/A$.

The parameter α is always positive. This can be easily seen for prolate spheroids ($a > 1$), since both contributions to (A 1) are positive. As regards oblate spheroids ($a < 1$), α could possibly become negative only if

$$\lambda < (1 - a^2) \cos^2 \theta_0 = \lambda_{a, \theta_0} \leq 1, \quad (\text{A } 3)$$

and it is therefore sufficient to examine the region $0 \leq a < 1$, $0 \leq \lambda < \lambda_{a, \theta_0}$. In this region however, we have

$$\alpha \geq (\lambda - 2)^2 \cos^2 \theta_0 - \max_{\substack{0 \leq a < 1, \\ 0 \leq \lambda < \lambda_{a, \theta_0}}} \left[\frac{\sin^2 \theta_0}{1 - (1 - a^2) \cos^2 \theta_0} ((1 - a^2) \cos^2 \theta_0 - \lambda) \right] \\ = \cos^2 \theta_0 ((\lambda - 2)^2 - 1) > 0 \quad \text{for } 0 \leq \lambda < \lambda_{a, \theta_0}. \quad (\text{A } 4)$$

Hence α is always positive for both prolate and oblate spheroids, as stated.

References

- Braams, C. M. 1952 On the influence of friction on the motion of a top. *Physica* **18**, 503–514.
- Childress, S. & Gilbert, A. D. 1995 *Stretch, twist, fold: the fast dynamo*. Springer
- Cohen, R. J. 1977 The tippe top revisited. *Am. J. Phys.* **45**, 12–17.
- Del Campo, A. R. 1955 Tippe top (topsy-turnee top) continued. *Am. J. Phys.* **23**, 544–545.
- Ebenfeld, S. & Scheck, F. 1995 A new analysis of the tippe top: asymptotic states and Liapunov stability. *Ann. Phys.* **243**, 195–217.
- Fokker, A. D. 1952 The tracks of top's pegs on the floor. *Physica* **18**, 497–502.
- Gray, C. G. & Nickel, B. G. 2000 Constants of the motion for nonslipping tippe tops and other tops with round pegs. *Am. J. Phys.* **68**, 821–828.
- Guckenheimer, J. & Holmes, P. 1983 *Nonlinear oscillations, dynamical systems, and bifurcations of vector fields*. Applied Mathematical Sciences, vol. 42. Springer.
- Hugenholtz, N. M. 1952 On tops rising by friction. *Physica* **18**, 515–527.
- Jellett, J. H. 1872 *A treatise on the theory of friction*, p. 185. London: Macmillan.

- Kane, T. R. & Levinson, D. A. 1978 A realistic solution of the symmetric top problem *J. Appl. Mech.* **45**, 903–908.
- Klopfenstein, R. W. 1971 Numerical differentiation formulas for stiff systems of ordinary differential equations. *RCA Review* **32**, 447–462.
- Mertens, R. & De Corte, L. 1978 An exact mathematical solution of the problem of tops rising by friction. *Z. Angew. Math. Mech.* **58**, T116–T118.
- Mertens, R., Hereman, W. & De Spiegeleere, R. 1982 On the exact theory of tops rising by friction. *Z. Angew. Math. Mech.* **62**, T58–T60.
- Moffatt, H. K. & Shimomura, Y. 2002 Spinning eggs: a paradox resolved. *Nature* **417**, 385–386.
- Murakami, C. 1995 All-passive-type rotary magnetic bearing system based on stability principle of sleeping tops. *JSME Int. J. C* **38**, 601–608.
- O'Brien, S. & Synge, J. L. 1954 The instability of the tippe top explained by sliding friction. *Proc. R. Irish Acad. A* **56**, 23–35.
- Or, A. C. 1994 The dynamics of a tippe top. *SIAM J. Appl. Math.* **54**, 597–609.
- Parkyn, D. G. 1958 The inverting top. *Math. Gazette* **40**, 260–265.
- Perry, J. 1957 *Spinning tops and gyroscopic motions*. New York: Dover.
- Saffman, P. G. 1992 *Vortex dynamics*. Cambridge University Press.
- Shampine, L. F. 1980 Implementation of implicit formulas for the solution of ODEs. *SIAM J. Sci. Statist. Comput.* **1**, 103–118.

As this paper exceeds the maximum length normally permitted,
the authors have agreed to contribute to production costs.